

# Instability windows and evolution of rapidly rotating neutron stars

Mikhail E. Gusakov<sup>1,2</sup>, Andrey I. Chugunov<sup>1</sup>, and Elena M. Kantor<sup>1</sup>

<sup>1</sup> *Ioffe Physical Technical Institute, Polytekhnicheskaya 26, 194021 St.-Petersburg, Russia*  
<sup>2</sup> *St.-Petersburg State Polytechnical University, Polytekhnicheskaya 29, 195251 St.-Petersburg, Russia*

We consider an instability of rapidly rotating neutron stars in low-mass X-ray binaries (LMXBs) with respect to excitation of  $r$ -modes (which are analogous to Earth’s Rossby waves controlled by the Coriolis force). We argue that finite temperature effects in the superfluid core of a neutron star lead to a resonance coupling and enhanced damping (and hence stability) of oscillation modes at *certain* stellar temperatures. Using a simple phenomenological model we demonstrate that neutron stars with high spin frequency may spend a substantial amount of time at these ‘resonance’ temperatures. This finding allows us to explain puzzling observations of hot rapidly rotating neutron stars in LMXBs and to predict a new class of hot, non-accreting, rapidly rotating neutron stars, some of which may have already been observed and tentatively identified as quiescent LMXB (qLMXB) candidates. We also impose a new *theoretical* limit on the neutron star spin frequency, explaining the cut-off spin frequency  $\sim 730$  Hz, following from the statistical analysis of accreting millisecond X-ray pulsars. Besides explaining the observations, our model provides a new tool to constrain superdense matter properties comparing measured and theoretically predicted resonance temperatures.

*Introduction.*— Neutron stars (NSs) are rotating compact objects. Rotation allows NSs to support the modes restored by the Coriolis force, the so-called *inertial* oscillation modes, including  $r$ -modes [1]. The  $r$ -modes, neglecting dissipation, are subject to gravitationally driven instability at *any* NS spin frequency  $\nu$  [2]; the most unstable are  $r$ -modes with low multipolarities ( $m = 2, 3$ ). Correspondent timescales,  $\tau_{\text{GR}} < 0$ , can be estimated analytically [1, 3]. Dissipation suppresses the instability to some extent; at temperatures of interest, dissipation timescales,  $\tau_{\text{Diss}} > 0$ , for  $r$ -modes are given by the shear viscosity. As a result, the star is predicted to be unstable with respect to  $r$ -modes within the “instability window”, that is a region of spin frequency  $\nu$  and redshifted internal stellar temperature ( $T^\infty$ ), where  $1/\tau_{\text{GR}} + 1/\tau_{\text{Diss}} < 0$  [1]. For NSs observed in this region the  $r$ -mode amplitude should increase exponentially. An amplified  $r$ -mode rapidly heats up the star (by dissipation) and brakes stellar rotation transmitting angular momentum to gravitational radiation [4]. Therefore, the star should quickly leave the instability window, making vanishingly small the probability to observe it unstable. However, some of NSs, which are observed in low-mass X-ray binaries (LMXBs; LMXB is a binary system consisting of an NS and a low-mass companion star, which fills the Roche lobe) fall well outside the stability region [5, 6]. Even additional dissipation mechanisms (Ekman layer, bulk viscosity, etc.) hardly explain the fastest and warmest sources [5–7] without appeal to an exotic NS composition (e.g., Ref. [8]), strong vortex pinning at the base of the NS crust [9] or rather strong ( $> 10^{11}$  G) radial magnetic field at the crust-core boundary [9, 10], which is much larger than typical surface magnetic field of NSs in LMXBs  $\sim 10^8$  G.

Furthermore, it is generally believed that LMXBs are progenitors of the fastest rotating stars – millisecond pulsars [11]. They supposed to be spun up by accretion,

but the  $r$ -mode instability can limit their spin frequency [12, 13] at  $\nu \sim 300 - 400$  Hz, making an interpretation of the faster pulsars (such as PSR J1748-2446ad rotating at 716 Hz [14]) very difficult.

To overcome these difficulties, we propose a phenomenological model, whose cornerstone is superfluidity of neutrons in the NS core. Theoretical calculations predict that at temperatures  $T^\infty \lesssim 10^8 \div 10^9$  K neutrons in the core are superfluid [15], which is confirmed by observations of cooling isolated NSs [16–19].  $r$ -modes, described above, generally are not greatly affected by superfluidity [20]. They correspond to the comoving oscillations of normal component (electrons and Bogoliubov excitations of baryons) and superfluid component (paired neutrons) of the matter; we will call them *normal* modes. However, similarly to the second sound in superfluids [21, 22], an additional class of inertial modes exists in superfluid stars, – *superfluid* modes ( $i^s$ -modes), which are counter-moving oscillations of normal and superfluid matter components [20, 23]. Strictly speaking,  $i^s$  and  $r$ -modes are clearly distinct only if one sets to zero the so-called *coupling parameter*  $s$  [24–26]. In this approximation the spectrum and eigenfunctions of the normal modes coincide with the corresponding quantities of a nonsuperfluid star and do not depend on temperature. On the contrary, the eigenfrequencies of superfluid modes strongly depend on  $T^\infty$  [27, 28]. In reality, the actual coupling parameter  $s$  is although small but finite, and depends on the equation of state and properties of the modes [29]. This leads to a strong interaction (*mixing*) of  $r$  and  $i^s$ -modes when their frequencies become close to one another. Then the avoided crossing of modes occurs in the  $\omega - T^\infty$  plane [see Fig. 1(a)], similar to avoided crossings of electron terms in molecules (see, e.g., Ref. [30], §79). The avoided crossings of oscillation modes are typical for stellar oscillations [23, 25, 31]; their existence for  $r$ -mode and  $i^s$ -modes is the main ingredient of our

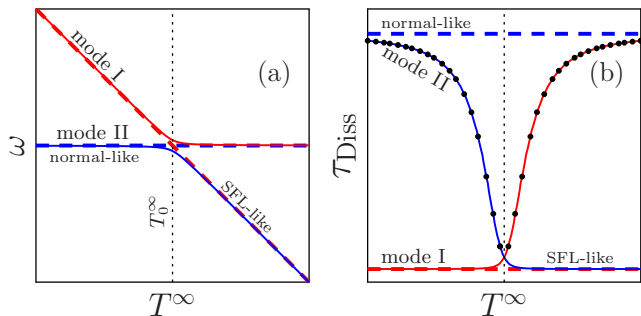


FIG. 1: (color online) A scheme of avoided crossing of  $r$ -mode with  $i^s$ -mode. Oscillation frequency  $\omega$  [panel (a)], and  $\tau_{\text{Diss}}$  [panel (b)] versus temperature  $T^\infty$  for two oscillation modes (I and II) of a superfluid NS, experiencing avoided crossing at  $T^\infty = T_0^\infty$ . Dashes correspond to an approximation of independent oscillation modes, solid lines show the exact solution allowing for the interaction of modes I and II. Vertical dotted lines indicate  $T_0^\infty$ . Filled circles in the panel (b) illustrate enhanced damping of  $r$ -mode-like oscillations near  $T^\infty = T_0^\infty$ .

phenomenological model.

*Observational data.*— Spin frequencies  $\nu$  and quiescent effective redshifted surface temperatures  $T_{\text{eff}}^\infty$  are known for 20 neutron stars in LMXBs [32–49]. Following Ref. [6] we calculate internal redshifted temperatures  $T^\infty$  for each source assuming thermally relaxed crust. The range of temperatures corresponding to possible envelope compositions is shown by error bars in Figs. 2, 3; the filled circles correspond to fiducial composition (see also supplemented table in [50]). Many of the rapidly rotating warm sources fall well outside the stability region [above the dashed curve in Fig. 2(b)] plotted neglecting resonance coupling of  $i^s$  and  $r$ -modes ( $s = 0$  approximation).

*Mode dissipation in  $s = 0$  approximation.*— In this case, for  $r$ -modes the dissipation timescale can be written as  $\tau_{\text{Diss}}^r = \tau_{\text{S}}/\kappa_m \approx \tau_{\text{S}0} (T_8^\infty)^2/\kappa_m$ , where  $\tau_{\text{S}}$  describes dissipation due to the electron shear viscosity [51] and  $\kappa_m$  is a dimensionless coefficient which models the present uncertainties in the knowledge of shear viscosity [51–54], and effects of other dissipation mechanisms (such as Ekman layer dissipation [1, 55]). Here  $T_8^\infty \equiv T^\infty/(10^8 \text{ K})$ ;  $\tau_{\text{S}0} \approx 2.2 \times 10^5 \text{ s}$  for  $m = 2$   $r$ -mode and  $\tau_{\text{S}0} \approx 1.2 \times 10^5 \text{ s}$  for  $m = 3$   $r$ -mode [29]. To describe observations, for  $m = 3$   $r$ -mode we take  $\kappa_3 = 5$  as a fiducial value. For  $m = 2$   $r$ -mode we choose  $\kappa_2 = 1$ , but larger or lower values are also acceptable for our scenario. For  $i^s$ -modes damping is very strong [23] due to extremely effective *mutual friction* mechanism, that tends to equalize the velocities of normal and superfluid components [56]. The corresponding timescale is  $\tau_{\text{Diss}}^{\text{SFL}} \approx \tau_{\text{MF}0}(1 \text{ kHz}/\nu)$ ,  $\tau_{\text{MF}0} \approx 4.7 \text{ s}$  [23]. Concerning gravitational radiation timescales, for  $r$ -modes one has  $\tau_{\text{GR}}^r \approx \tau_{\text{GR}0}(\nu/1 \text{ kHz})^{-2m-2}$  [1, 3] (where  $\tau_{\text{GR}0} \approx -46.4 \text{ s}$  and  $-1250 \text{ s}$  for  $m = 2$  and  $m = 3$   $r$ -modes, respectively). For  $i^s$ -modes gravitational radi-

ation is suppressed in comparison to  $r$ -modes by a factor  $c_{\text{GR}} \gtrsim 10^4$  [20, 23]. For readability of Fig. 2(a) we take  $\tau_{\text{GR}}^{\text{SFL}} \approx c_{\text{GR}}\tau_{\text{GR}}^r$ , with  $c_{\text{GR}} = 100$ . We checked that any  $c_{\text{GR}} \gtrsim 1$  does not affect our results. In  $s = 0$  approximation, a crossing of modes takes place in  $\omega - T^\infty$  plane (see the dashed lines in Fig. 1(a)); in that case superfluid and normal modes would not ‘feel’ each other and the damping time scales do not have any features associated with resonant coupling of modes [see the dashed lines in Fig. 1(b)].

*Avoided crossings and dissipation of modes.*— In reality, coupling of the superfluid and normal modes near avoided crossings dramatically modifies the dissipation properties of an oscillating star. Instead of crossings of these modes in the  $\omega - T^\infty$  plane, one has avoided crossings: As  $T^\infty$  varies, superfluid mode turns into the normal mode and vice versa (see Fig. 1). For example, the mode II in Fig. 1(a) behaves as normal  $r$ -mode (normal-like) at low  $T^\infty$  and as a superfluid  $i^s$ -mode (SFL-like) at high  $T^\infty$ . Correspondingly, its dissipation timescale  $\tau_{\text{Diss}}$  should smoothly vary from the high  $r$ -mode value at  $T^\infty < T_0^\infty$  (weak dissipation) to the low value in  $i^s$ -mode-like regime at  $T^\infty > T_0^\infty$  (strong dissipation). For the mode I the behavior of  $\tau_{\text{Diss}}(T^\infty)$  is opposite [see Fig. 1(b) for illustration]. The crucial thing about the scenario proposed in the present note is that  $\tau_{\text{Diss}}$  should differ substantially before ( $T^\infty < T_0^\infty$ ) and after ( $T^\infty > T_0^\infty$ ) an avoided crossing, while the actual form of the function  $\tau_{\text{Diss}}(T^\infty)$  at  $T^\infty \sim T_0^\infty$  is not important. Bearing this in mind, in all numerical calculations we use a simple phenomenological model of the mode mixing evoked by the perturbation theory of quantum mechanics. Within this model the damping ( $X = \text{Diss}$ ) and gravitational radiation ( $X = \text{GR}$ ) timescales for the modes I and II are given, respectively, by

$$\tau_{\text{X}I}^{-1} \approx \sin^2 \theta(x)/\tau_{\text{X}}^r + \cos^2 \theta(x)/\tau_{\text{X}}^{\text{SFL}}, \quad (1)$$

$$\tau_{\text{X}II}^{-1} \approx \cos^2 \theta(x)/\tau_{\text{X}}^r + \sin^2 \theta(x)/\tau_{\text{X}}^{\text{SFL}} \quad (2)$$

(see Ref. [29] for more details). Here  $\theta(x) = [\pi/2 + \arctan(x)]/2$  and  $x \equiv (T^\infty - T_0^\infty)/\Delta T^\infty$ ; the parameter  $\Delta T^\infty$  determines the width of the avoided crossing.

The qualitative behavior of oscillation modes in superfluid NSs described above has been confirmed by direct calculation of oscillation modes in nonrotating NSs [25, 27, 28, 57]. They demonstrate a large number of resonances [well described by Eqs. (1) and (2)] between the normal and superfluid modes, which occur at  $T^\infty \sim (0.1 - 1)T_{\text{cn}}^\infty$ , where  $T_{\text{cn}}^\infty$  is a typical neutron critical temperature (at  $T^\infty \lesssim 0.1T_{\text{cn}}^\infty$  we have no avoided crossings because SFL hydrodynamics is then independent of temperature). Our model is also supported by the figure 12 of Lee and Yoshida [20]. These authors employed the zero temperature approximation ( $T^\infty = 0$ ) and varied the so-called ‘entrainment’ parameter  $\eta$ , that parameterizes interaction between the superfluid neutrons and superconducting protons. It follows from the microphysics

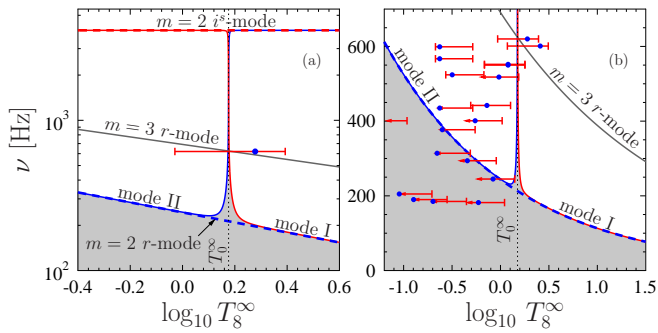


FIG. 2: (color online) An example of instability window for superfluid NS. The star is stable in the grey region, while the white region is the instability window, splitted up by the ‘stability peak’ at  $T^\infty \approx T_0^\infty$ . The solid curves correspond to instability curves for  $m = 2$  modes I and II, respectively, which experience avoided crossing at  $T_0^\infty = 1.5 \times 10^8$  K. The dashed curves correspond to  $m = 2$   $r$ - and  $i^s$ -modes [panel (a) only], plotted under the assumption that they are completely decoupled. The grey line is the instability curve for  $m = 3$   $r$ -mode, plotted ignoring the resonance coupling with superfluid modes. The temperature  $T_0^\infty$  is shown by the vertical dotted line. Panel (b) shows frequencies and temperatures of the observed sources [50]. Only the fastest spinning source 4U 1608-522 is shown in panel (a).

calculations [58–60] that  $\eta$  is a function of  $T^\infty$ . Hence, its variation is *analogous* to a variation of stellar temperature. Figure 12 of Ref. [20] shows the dissipation timescale  $\tau_{\text{MF}}^r$  due to mutual friction for  $m = 2$   $r$ -mode (or, more accurately, for the oscillation mode which mimics  $r$ -mode) as a function of  $\eta$ . One can see that  $\tau_{\text{MF}}^r$  sharply decreases (by few orders of magnitude) at exactly the same values of  $\eta$  at which one observes the resonances between  $r$ - and  $i^s$ -modes in their figure 8, confirming thus our model. Near the resonances  $r$ -mode starts to transform into  $i^s$ -mode, and hence  $\tau_{\text{MF}}^r$  drops down rapidly. Moving away from the avoided crossing (by decreasing or increasing  $\eta$ ), the solution found by Lee and Yoshida resembles more and more  $m = 2$   $r$ -mode. Consequently,  $\tau_{\text{MF}}^r$  grows on both sides of the resonance, approaching the asymptote value corresponding to the pure (with no admixture of  $i^s$ -mode)  $m = 2$   $r$ -mode [see filled circles in Fig. 1(b)].

*Realistic instability windows.*– The avoided crossings of modes dramatically modify the instability window. For instance, assume that modes I and II experience an avoided crossing at  $T^\infty = T_0^\infty = 1.5 \times 10^8$  K. Their instability curves, given by the condition  $1/\tau_{\text{GR}} + 1/\tau_{\text{Diss}} = 0$ , are shown in Fig. 2(a,b) by solid lines. To plot the curves we used Eqs.(1) and (2) and set  $\Delta T^\infty = 10^{-3} T_0^\infty$ . The panel (b) is a version of panel (a), but plotted in a different scale. In addition, Fig. 2(a,b) shows the instability curves for: (i)  $m = 3$   $r$ -mode; (ii)  $m = 2$   $r$ -mode; (iii) superfluid  $i^s$ -mode [panel (a) only]. The latter curves (i)–(iii) are obtained using  $s = 0$  approximation. As ex-

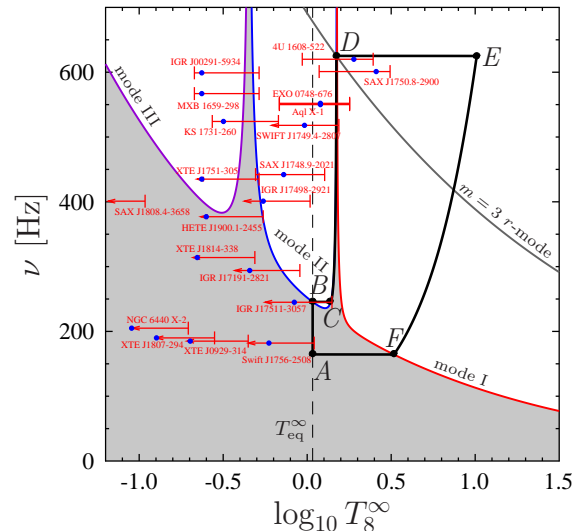


FIG. 3: (color online) An example of evolutionary track of an NS in LMXB. The evolution track  $ABCDEF A$  is shown by solid line. The solid curves are instability curves for  $m = 2$  modes I, II, and III, respectively; they experience avoided crossing at  $T_0^\infty = 4.5 \times 10^7$  K (modes III and II) and  $1.5 \times 10^8$  K (modes II and I). Other notations are the same as in Fig. 2.

pected, far from the avoided crossing the solid (modes I and II) and dashed ( $r$ - and  $i^s$ -modes) lines almost coincide. The instability window (at least one mode is unstable; white region) is splitted up by the ‘stability peak’ at  $T^\infty \approx T_0^\infty$  [61]. This is an inherent feature of  $r$ - and  $i^s$ -mode avoided crossing. In this region the instability curves of modes I and II continuously change their behavior from  $i^s$ -mode-like asymptote to  $r$ -mode-like one and vice versa. Therefore, for both modes the instability occurs at larger frequency, than for pure  $m = 2$   $r$ -mode. The most unstable mode at  $T^\infty = T_0^\infty$  is  $m = 3$   $r$ -mode; it determines the stability peak height. In reality, an  $r$ -mode can experience more than one avoided crossing with the superfluid modes [20, 25, 27, 28]. Unfortunately, the resonant temperatures  $T_0^\infty$  have not yet been calculated directly; here we treat them as free parameters to be inferred from observations. In Fig. 3 we demonstrate the instability windows for two avoided crossings of  $r$ -mode with  $i^s$ -modes – at  $T^\infty = 4.5 \times 10^7$  K and  $T^\infty = 1.5 \times 10^8$  K.

*NS evolution in LMXB.*– Dramatic modification of the instability window alters the evolution of an NS in LMXB. Corresponding equations were derived in Ref. [29] and are similar to those obtained in Refs. [62, 63] in the absence of  $i^s$ -modes. They follow from (i) angular momentum conservation, (ii) thermal balance of the star, and (iii) evolution of each mode owing to damping mechanisms and excitation by gravitational radiation. The solution to these equations results in the evolution track

*ABCDEF*A, shown by thick solid line in Fig. 3 (see Ref. [29] for more details). At the stage *AB* the star spins up by accretion while temperature stays constant,  $T^\infty = T_{\text{eq}}^\infty$ , owing to balance between cooling processes (neutrino emission from the bulk of the star and thermal electromagnetic radiation from its surface) and the accretion driven stellar heating [64]. Being pushed into the instability window by accretion spin up, the star is rapidly heated up by excited mode II and reaches the foot of the stability peak in point *C*. (Note that, for certain parameters of the model a star can execute the standard ‘Levin cycle’ [4] before reaching the point *C*.) At point *C* the (average) amplitude  $\alpha_{\text{eq}}$  of the mode II adjusts itself so as to ‘stick’ the star to the boundary of the stability peak (as in Refs. [29, 65–68]). Then two alternatives are possible. If gravitational wave torque corresponding to  $\alpha_{\text{eq}}$  is larger than accretion torque, the star will move downwards [65]; otherwise the star will climb up the peak [29, 67]. For realistic model parameters adopted here (see Ref. [29] for details) the second possibility is realized and the star reaches the point *D* [69]. In point *D* the star rushes into the instability window, where the instability of modes I and  $m = 3$  *r*-mode converts rotation energy of the star to gravitational waves and heat, and brings rapidly the star back to the stability region in point *F*. Then the star cools down to point *A* and cycle repeats. The NS spends most of the time climbing up the stability peak (stage *CD*), i.e. in the region which is thought to be unstable and unreachable in standard scenario (i.e., neglecting resonance coupling of *r*- and *i*<sup>s</sup>-modes) [4]. Thus, it is not surprising in our model that we see a number of stars (4U 1608-522, SAX J1750.8-2900, EXO 0748-676, Aql X-1, and SWIFT J1749.4-2807) at this stage.

Moreover, the low temperature sources IGR J00291-5934, MXB 1659-298, KS 1731-260, and XTE J1751-305 can not have  $T_{\text{eq}}^\infty$  larger than that corresponding to their measured temperatures. If it is low enough, the evolution track goes along the left edge of low-temperature stability peak, corresponding to the avoided crossing of the modes II and III (see Fig. 3), thus explaining high spin frequencies of these sources. The rest of the stars lie in the stability region, so they can be explained as going through stage *AB* of their evolution cycle.

*Discussion and conclusions.*— Our simple model naturally explains rapidly rotating NSs in LMXBs within the same assumptions as those adopted in ‘minimal cooling’ scenarios of Refs. [17, 71] (we note that these scenarios turn out to be very successful in interpretation of observations of cooling isolated NSs [16, 18, 19]). Furthermore, we predict spin frequencies of NSs to be limited by the height of the stability peak, defined by the instability of the  $m = 3$  *r*-mode, but not by  $m = 2$  *r*-mode, as it is usually assumed [6, 72]. This result explains the abrupt observational cut-off of the spin frequency distribution of accreting millisecond pulsars above  $\sim 730$  Hz [73, 74]. In addition, we predict that the main heating mechanism for

the stars climbing up the stability peak (the most rapidly rotating warm NSs) is vibrational dissipation, but not accretion, as it is usually supposed [64].

Moreover, these NSs will remain attached to the stability peak *CD* (and hence stay warm) even after accretion will be stopped due to, e.g., depletion of the low-mass companion. Then, according to our scenario, they will start to spin down slowly (during  $10^8$ – $10^9$  years) because of gravitational and magneto-dipole radiation. Such NSs should be observed as X-ray sources with purely thermal NS atmosphere spectrum, and hence should have similar observational properties as quiescent LMXB (qLMXB) candidates [75, 76]. This means that some of X-ray sources known as qLMXB candidates, which have never been observed in outbursts [76], can in fact be heated not by accretion (as is the case for qLMXBs), but by vibrational dissipation. We propose to call these objects ‘HOFNARs’ (from HOT and Fast Non-Accreting Rotators) or ‘hot widows’ (in analogy with the name ‘black widows’ denoting millisecond pulsars with ablating companions). Note that, HOFNARs should appear not only in our scenario, but in *any* evolutionary scenario, which assumes that hot rapidly rotating NSs in LMXBs are located in the instability window in some (quasi)stationary state (including low-saturation-amplitude scenarios, see, e.g., Refs. [77, 78]).

The temperatures of hot rapidly rotating NSs (both accreting and non-accreting) must coincide with the resonance temperatures  $T_0^\infty$ . The resonance temperatures, we extract from observations of LMXBs ( $\sim 4.5 \times 10^7$  K –  $1.5 \times 10^8$  K), provide a rough estimate for neutron critical temperature  $T_{\text{cn}}^\infty$  around  $2 \times 10^8$  K  $\lesssim T_{\text{cn}}^\infty \lesssim 8 \times 10^8$  K (neutrons should be superfluid at high temperature resonance, but  $T_{\text{cn}}^\infty$  should not be too high to guarantee temperature dependence of *i*<sup>s</sup>-mode frequency at low temperature resonance), in agreement with theoretical predictions [15] and constraints imposed by ‘minimal cooling’ scenarios [16–19]. Accurate calculations of resonance temperatures and new observational data from future space missions such as SRG [79], NICER [80], and LOFT [81] will put much more stringent constraints on the properties of superdense matter and parameters of superfluidity.

*Acknowledgments.*— We are grateful to A. D. Kaminker, O. Y. Kargaltsev, G. G. Pavlov, A. Y. Potekhin, Y. A. Shibano, A. I. Tsygan, V. A. Urpin, D. G. Yakovlev, D. A. Zyuzin for insightful comments and discussions, and to O. V. Zakutnyaya for assistance in preparation of the manuscript. This work was partially supported by RF president programme (grants MK-857.2012.2, MK-506.2014.2, and NSh-4035.2012.2), by RFBR (grants 11-02-00253-a, 12-02-31270-mol-a, and 14-02-31616-mol-a) by the Dynasty Foundation, and by the Ministry of Education and Science of Russian Federation (Agreement No. 8409, 2012).

- 
- [1] N. Andersson and K. D. Kokkotas, *International Journal of Modern Physics D* **10**, 381 (2001), arXiv:gr-qc/0010102.
- [2] N. Andersson, *Astrophys. J.* **502**, 708 (1998), arXiv:gr-qc/9706075.
- [3] L. Lindblom, B. J. Owen, and S. M. Morsink, *Physical Review Letters* **80**, 4843 (1998), arXiv:gr-qc/9803053.
- [4] Y. Levin, *Astrophys. J.* **517**, 328 (1999), arXiv:astro-ph/9810471.
- [5] W. C. G. Ho, N. Andersson, and B. Haskell, *Physical Review Letters* **107**, 101101 (2011), 1107.5064.
- [6] B. Haskell, N. Degenaar, and W. C. G. Ho, *Mon. Not. R. Astron. Soc.* **424**, 93 (2012), 1201.2101.
- [7] N. Andersson, J. Baker, K. Belczynski, S. Bernuzzi, E. Berti, L. Cadonati, P. Cerdá-Durán, J. Clark, M. Favata, L. S. Finn, et al., *Classical and Quantum Gravity* **30**, 193002 (2013), 1305.0816.
- [8] G. Rupak and P. Jaikumar, *Phys. Rev. C* **88**, 065801 (2013), 1209.4343.
- [9] J. B. Kinney and G. Mendell, *Phys. Rev. D* **67**, 024032 (2003), gr-qc/0206001.
- [10] G. Mendell, *Phys. Rev. D* **64**, 044009 (2001), gr-qc/0102042.
- [11] M. A. Alpar, A. F. Cheng, M. A. Ruderman, and J. Shaham, *Nature (London)* **300**, 728 (1982).
- [12] N. Andersson, K. Kokkotas, and B. F. Schutz, *Astrophys. J.* **510**, 846 (1999), arXiv:astro-ph/9805225.
- [13] N. Andersson, K. D. Kokkotas, and N. Stergioulas, *Astrophys. J.* **516**, 307 (1999), arXiv:astro-ph/9806089.
- [14] J. W. T. Hessels, S. M. Ransom, I. H. Stairs, P. C. C. Freire, V. M. Kaspi, and F. Camilo, *Science* **311**, 1901 (2006), arXiv:astro-ph/0601337.
- [15] J. M. Dong, U. Lombardo, and W. Zuo, *Phys. Rev. C* **87**, 062801 (2013), 1304.0117.
- [16] M. E. Gusakov, A. D. Kaminker, D. G. Yakovlev, and O. Y. Gnedin, *Mon. Not. R. Astron. Soc.* **363**, 555 (2005), arXiv:astro-ph/0507560.
- [17] D. Page, J. M. Lattimer, M. Prakash, and A. W. Steiner, *Astrophys. J. Suppl. Ser.* **155**, 623 (2004), arXiv:astro-ph/0403657.
- [18] P. S. Shternin, D. G. Yakovlev, C. O. Heinke, W. C. G. Ho, and D. J. Patnaude, *Mon. Not. R. Astron. Soc.* **412**, L108 (2011).
- [19] D. Page, M. Prakash, J. M. Lattimer, and A. W. Steiner, *Phys. Rev. Lett.* **106**, 081101 (2011).
- [20] U. Lee and S. Yoshida, *Astrophys. J.* **586**, 403 (2003), arXiv:astro-ph/0211580.
- [21] I. M. Khalatnikov, *An Introduction to the Theory of Superfluidity* (Addison-Wesley, New York, 1989).
- [22] L. A. Sidorenkov, M. K. Tey, R. Grimm, Y.-H. Hou, L. Pitaevskii, and S. Stringari, *Nature* **498**, 78 (2013).
- [23] S. Yoshida and U. Lee, *Mon. Not. R. Astron. Soc.* **344**, 207 (2003), arXiv:astro-ph/0302313.
- [24] M. E. Gusakov and E. M. Kantor, *Phys. Rev. D* **83**, 081304 (2011), 1007.2752.
- [25] M. E. Gusakov, E. M. Kantor, A. I. Chugunov, and L. Gualtieri, *Mon. Not. R. Astron. Soc.* **428**, 1518 (2013), 1211.2452.
- [26] E. M. Kantor and M. E. Gusakov, in *Electromagnetic Radiation from Pulsars and Magnetars*, edited by W. Lewandowski, O. Maron, and J. Kijak (2013), vol. 466 of *Astronomical Society of the Pacific Conference Series*, p. 211.
- [27] E. M. Kantor and M. E. Gusakov, *Phys. Rev. D* **83**, 103008 (2011), 1105.4040.
- [28] A. I. Chugunov and M. E. Gusakov, *Mon. Not. R. Astron. Soc.* **418**, L54 (2011), 1107.4242.
- [29] M. E. Gusakov, A. I. Chugunov, and E. M. Kantor, *ArXiv e-prints* (2013), 1305.3825.
- [30] L. Landau and E. Lifshits, *Quantum Mechanics: Non-Relativistic Theory* (Butterworth-Heinemann Limited, 1977), ISBN 9780750635394, URL <http://books.google.ru/books?id=J9ui6KwC4mMC>.
- [31] C. Aerts, J. Christensen-Dalsgaard, and D. W. Kurtz, *Asteroseismology* (Springer Science+ Business Media, 2010).
- [32] A. Patruno, *Astrophys. J.* **722**, 909 (2010), 1006.0815.
- [33] A. Patruno and A. L. Watts, *ArXiv e-prints* (2012), 1206.2727.
- [34] R. Wijnands, T. Strohmayer, and L. M. Franco, *Astrophys. J. Lett.* **549**, L71 (2001), arXiv:astro-ph/0008526.
- [35] C. O. Heinke, D. Altamirano, H. N. Cohn, P. M. Lugger, S. A. Budac, M. Servillat, M. Linares, T. E. Strohmayer, C. B. Markwardt, R. Wijnands, et al., *Astrophys. J.* **714**, 894 (2010), 0911.0444.
- [36] E. M. Cackett, R. Wijnands, C. O. Heinke, P. D. Edmonds, W. H. G. Lewin, D. Pooley, J. E. Grindlay, P. G. Jonker, and J. M. Miller, *Astrophys. J.* **620**, 922 (2005), arXiv:astro-ph/0407448.
- [37] N. Degenaar, A. Patruno, and R. Wijnands, *Astrophys. J.* **756**, 148 (2012), 1204.6059.
- [38] E. M. Cackett, E. F. Brown, A. Cumming, N. Degenaar, J. M. Miller, and R. Wijnands, *Astrophys. J. Lett.* **722**, L137 (2010), 1008.4727.
- [39] M. P. Muno, D. W. Fox, E. H. Morgan, and L. Bildsten, *Astrophys. J.* **542**, 1016 (2000), arXiv:astro-ph/0003229.
- [40] E. M. Cackett, J. K. Fridriksson, J. Homan, J. M. Miller, and R. Wijnands, *Mon. Not. R. Astron. Soc.* **414**, 3006 (2011), 1102.5016.
- [41] N. Degenaar, M. T. Wolff, P. S. Ray, K. S. Wood, J. Homan, W. H. G. Lewin, P. G. Jonker, E. M. Cackett, J. M. Miller, E. F. Brown, et al., *Mon. Not. R. Astron. Soc.* **412**, 1409 (2011), 1007.0247.
- [42] E. M. Cackett, R. Wijnands, J. M. Miller, E. F. Brown, and N. Degenaar, *Astrophys. J. Lett.* **687**, L87 (2008), 0806.1166.
- [43] A. L. Watts, *Ann. Rev. Astron. Astrophys.* **50**, 609 (2012), 1203.2065.
- [44] A. L. Watts, B. Krishnan, L. Bildsten, and B. F. Schutz, *Mon. Not. R. Astron. Soc.* **389**, 839 (2008), 0803.4097.
- [45] R. Wijnands, J. Homan, C. O. Heinke, J. M. Miller, and W. H. G. Lewin, *Astrophys. J.* **619**, 492 (2005), arXiv:astro-ph/0406057.
- [46] C. O. Heinke, P. G. Jonker, R. Wijnands, C. J. Deloye, and R. E. Taam, *Astrophys. J.* **691**, 1035 (2009), 0810.0497.
- [47] C. O. Heinke, P. G. Jonker, R. Wijnands, and R. E. Taam, *Astrophys. J.* **660**, 1424 (2007), arXiv:astro-ph/0612232.
- [48] A. W. Lowell, J. A. Tomsick, C. O. Heinke, A. Bodaghee, S. E. Boggs, P. Kaaret, S. Chaty, J. Rodriguez, and R. Walter, *Astrophys. J.* **749**, 111 (2012), 1202.1531.
- [49] R. E. Rutledge, L. Bildsten, E. F. Brown, G. G. Pavlov, and V. E. Zavlin, *Astrophys. J.* **514**, 945 (1999), arXiv:astro-ph/9810288.

- [50] See supplementary information (p. 7) for the table summarizing observational data and internal temperatures of neutron stars in low-mass X-ray binaries.
- [51] P. S. Shternin and D. G. Yakovlev, *Phys. Rev. D* **78**, 063006 (2008), 0808.2018.
- [52] O. Benhar and M. Valli, *Physical Review Letters* **99**, 232501 (2007), 0707.2681.
- [53] H. F. Zhang, U. Lombardo, and W. Zuo, *Phys. Rev. C* **82**, 015805 (2010), 1006.2656.
- [54] P. S. Shternin, M. Baldo, and P. Haensel, *Phys. Rev. C* **88**, 065803 (2013).
- [55] M. Rieutord, *Astrophys. J.* **550**, 443 (2001).
- [56] M. A. Alpar, S. A. Langer, and J. A. Sauls, *Astrophys. J.* **282**, 533 (1984).
- [57] M. E. Gusakov and N. Andersson, *Mon. Not. R. Astron. Soc.* **372**, 1776 (2006).
- [58] M. E. Gusakov and P. Haensel, *Nuclear Physics A* **761**, 333 (2005), arXiv:astro-ph/0508104.
- [59] M. E. Gusakov, E. M. Kantor, and P. Haensel, *Phys. Rev. C* **80**, 015803 (2009).
- [60] M. E. Gusakov, *Phys. Rev. C* **81**, 025804 (2010), 1001.4452.
- [61] Generally,  $T_0^\infty$  can be a function of  $\nu$ . This could make the stability peak a little bit curved, but would not affect our main conclusions.
- [62] B. J. Owen, L. Lindblom, C. Cutler, B. F. Schutz, A. Vecchio, and N. Andersson, *Phys. Rev. D* **58**, 084020 (1998), arXiv:gr-qc/9804044.
- [63] W. C. G. Ho and D. Lai, *Astrophys. J.* **543**, 386 (2000), arXiv:astro-ph/9912296.
- [64] E. F. Brown, L. Bildsten, and R. E. Rutledge, *Astrophys. J. Lett.* **504**, L95 (1998), arXiv:astro-ph/9807179.
- [65] N. Andersson, D. I. Jones, and K. D. Kokkotas, *Mon. Not. R. Astron. Soc.* **337**, 1224 (2002).
- [66] R. V. Wagoner, *Astrophys. J. Lett.* **578**, L63 (2002).
- [67] A. Reisenegger, and A. Bonačić, *Physical Review Letters* **91**, 201103 (2003).
- [68] M. Nayyar, and B. J. Owen, *Phys. Rev. D* **73**, 084001 (2006).
- [69] In principle, for sufficiently high magnetic fields an NS can reach spin equilibrium [70] (when accretion torque balances gravitational and magneto-dipole torques) before approaching the point D. In that case it will stay in ‘equilibrium’ point at the peak CD until the end of accretion epoch, so that the cycle ABCDEFA will never be completed (see Ref. [29] for more details).
- [70] S. A. Rappaport, J. M. Fregeau, and H. Spruit, *Astrophys. J.* **606**, 436 (2004), arXiv:astro-ph/0310224.
- [71] M. E. Gusakov, A. D. Kaminker, D. G. Yakovlev, and O. Y. Gnedin, *Astron. Astrophys.* **423**, 1063 (2004), arXiv:astro-ph/0404002.
- [72] L. Bildsten, *Astrophys. J. Lett.* **501**, L89 (1998), arXiv:astro-ph/9804325.
- [73] D. Chakrabarty, E. H. Morgan, M. P. Muno, D. K. Galloway, R. Wijnands, M. van der Klis, and C. B. Markwardt, *Nature (London)* **424**, 42 (2003), arXiv:astro-ph/0307029.
- [74] D. Chakrabarty, in *American Institute of Physics Conference Series*, edited by R. Wijnands, D. Altamirano, P. Soleri, N. Degenaar, N. Rea, P. Casella, A. Patruno, and M. Linares (2008), vol. 1068 of *American Institute of Physics Conference Series*, pp. 67–74, 0809.4031.
- [75] C. O. Heinke, J. E. Grindlay, P. M. Lugger, H. N. Cohn, P. D. Edmonds, D. A. Lloyd, and A. M. Cool, *Astrophys. J.* **598**, 501 (2003), arXiv:astro-ph/0305445.
- [76] S. Guillot, R. E. Rutledge, E. F. Brown, G. G. Pavlov, and V. E. Zavlin, *Astrophys. J.* **738**, 129 (2011), 1104.3864.
- [77] S. Mahmoodifar and T. Strohmayer, *Astrophys. J.* **773**, 140 (2013), 1302.1204.
- [78] R. Bondarescu and I. Wasserman, *ArXiv e-prints* (2013), 1305.2335.
- [79] A. Merloni, P. Predehl, W. Becker, H. Böhringer, T. Boller, H. Brunner, M. Brusa, K. Dennerl, M. Freyberg, P. Friedrich, et al., *ArXiv e-prints* (2012), 1209.3114.
- [80] K. C. Gendreau, Z. Arzoumanian, and T. Okajima, in *Society of Photo-Optical Instrumentation Engineers (SPIE) Conference Series* (2012), vol. 8443 of *Society of Photo-Optical Instrumentation Engineers (SPIE) Conference Series*.
- [81] M. Feroci, L. Stella, M. Van der Klis, T.-L. Courvoisier, M. Hernanz, R. Hudec, A. Santangelo, D. Walton, A. Zdziarski, D. Barret, et al., *Experimental Astronomy* **34**, 415 (2012).

## Supplementary information

TABLE I: **Observational data and internal temperatures of neutron stars in low-mass X-ray binaries.** The source names are given in the first column. The second column presents the neutron-star spin frequencies  $\nu$  which are taken from Refs. [32, 33]. The third column summarizes observational data on neutron-star redshifted effective temperatures  $T_{\text{eff}}^{\infty}$  in the quiescent state. The corresponding values are taken from the papers quoted in the fourth column. In those papers the thermal component was fitted by the hydrogen atmosphere models with the fiducial value of the neutron-star mass  $M = 1.4M_{\odot}$ . The internal temperatures calculated under assumption of a fully accreted envelope  $T_{\text{acc}}^{\infty}$ , partially accreted envelope with a layer of accreted light elements down to a column depth of  $10^9 \text{ g cm}^{-2}$  (the same fiducial value has been adopted in Refs. [6]); the corresponding ‘fiducial’ temperature is  $T_{\text{fid}}^{\infty}$ ), and purely iron envelope  $T_{\text{Fe}}^{\infty}$  are shown in the fifth, sixth, and seventh column, respectively. Finally, the eighth column presents (if available) estimates of the *averaged* accretion rates  $\dot{M}$  onto neutron stars and the corresponding references (the ninth column). The averaging is performed over a long period of time, which includes both active and quiescent phases.

Source <sup>a</sup>	$\nu$ [Hz]	$\frac{T_{\text{eff}}^{\infty}}{10^6 \text{ K}}$	Ref.	$\frac{T_{\text{acc}}^{\infty}}{10^8 \text{ K}}$	$\frac{T_{\text{fid}}^{\infty}}{10^8 \text{ K}}$	$\frac{T_{\text{Fe}}^{\infty}}{10^8 \text{ K}}$	$\frac{\dot{M}}{M_{\odot}} [\text{yr}^{-1}]$	Ref.
4U 1608-522	620	1.51	[49]	0.93	1.90	2.47	$3.6 \times 10^{-10}$	[47]
SAX J1750.8-2900	601	1.72	[48]	1.18	2.57	3.11	$2 \times 10^{-10}$	[48]
IGR J00291-5934	599	0.63 <sup>b</sup>	[46]	0.21	0.24	0.52	$2.5 \times 10^{-12}$	[46]
MXB 1659-298	567 <sup>c</sup>	0.63	[42]	0.21	0.24	0.52	$1.7 \times 10^{-10}$	[47]
EXO 0748-676 <sup>d</sup>	552	1.26	[41]	0.68	1.20	1.79		
Aql X-1	550	1.26	[40]	0.68	1.20	1.79	$4 \times 10^{-10}$	[47]
KS 1731-260	524 <sup>e</sup>	0.73	[38]	0.27	0.32	0.67	$< 1.5 \times 10^{-9}$	[47]
SWIFT J1749.4-2807	518	$< 1.16$	[37]	0.59	0.96	1.54		
SAX J1748.9-2021	442	1.04	[36]	0.49	0.72	1.27	$1.8 \times 10^{-10}$	[47]
XTE J1751-305	435	$< 0.63^a$	[46]	0.21	0.24	0.52	$6 \times 10^{-12}$	[46]
SAX J1808.4-3658	401	$< 0.27^a$	[46]	0.05	0.05	0.11	$9 \times 10^{-12}$	[46]
IGR J17498-2921	401	$< 0.93$	[37]	0.41	0.55	1.04		
HETE J1900.1-2455	377	$< 0.65$	[6]	0.22	0.25	0.55		
XTE J1814-338	314	$< 0.61^a$	[46]	0.20	0.22	0.49	$3 \times 10^{-12}$	[46]
IGR J17191-2821	294	$< 0.86$	[6]	0.36	0.45	0.90		
IGR J17511-3057	245	$< 1.1$	[6]	0.54	0.84	1.40		
NGC 6440 X-2	205	$< 0.37$	[6]	0.09	0.09	0.20	$1.3 \times 10^{-12}$	[35]
XTE J1807-294	190	$< 0.45^a$	[46]	0.12	0.13	0.28	$< 8 \times 10^{-12}$	[46]
XTE J0929-314	185	$< 0.58$	[45]	0.19	0.20	0.45	$< 2 \times 10^{-11}$	[46]
Swift J1756-2508	182	$< 0.96$	[6]	0.43	0.59	1.10		

<sup>a</sup>In comparison to Refs. [6, 77] we add an additional source (IGR J17498-2921) and accretion rates to the table. We also correct misprint in the value of frequency of MXB 1659-298. As in Ref. [77] we treat temperatures in Table 2 of Refs. [46] as local surface temperatures, but not redshifted ones as in Ref. [6]. We also correct misprint for the source NGC 6440 in Table 3 of Ref. [77] (its frequency 205 Hz corresponds to NGC 6440 X-2 – the second LMXB in NGC 6440 [35], but the temperature is given for SAX J1748.9-2021 – another LMXB in NGC 6440 [36]).

<sup>b</sup>We treat the effective temperature from the table 2 of Ref. [46] as a local one to reproduce the thermal luminosity from that reference.

<sup>c</sup>According to Refs. [34, 43, 44]

<sup>d</sup>The radius of this source was fixed at 15.6 km in spectral fits of Ref. [41].

<sup>e</sup>According to Refs. [39, 43, 44]